



 Cite this: *RSC Adv.*, 2020, 10, 15493

# Enhanced energy efficiency for the complete mineralization of diclofenac by self-sequential ultrasound enhanced ozonation

 Zhen Chen,<sup>abd</sup> Shewei Yang,<sup>bd</sup> Yonghong Wang,<sup>bd</sup> Mingshan Zhu <sup>c</sup> and Chaohai Wei<sup>\*a</sup>

Diclofenac (DCF), an anti-biodegradable drug, needs to be post-treated after conventional biochemical treatment. In this paper, ultrasound enhanced ozonation (UEO) under different conditions was employed to degrade DCF. The results showed that DCF was completely degraded by UEO in 8 min and complete total organic carbon (TOC) removal occurred in 120 min. The generation of  $\cdot\text{OH}$  via UEO could be achieved through ozone decomposition,  $\text{H}_2\text{O}$  sonolysis, and ozone sonolysis, which contributed to the complete mineralization of DCF. The total amount of  $\cdot\text{OH}$  produced by 200 kHz UEO was 3.8 times higher than that of single ozonation plus single sonolysis in 120 min. Typical persistent intermediates of DCF, such as oxalic acid and oxamic acid, could be efficiently degraded by UEO. It was found that 60 min ozonation followed by 60 min UEO had the best mineralization energy efficiency (MEE) ( $113 \text{ mg (kW h)}^{-1}$ ) at the base of complete mineralization and there was one-third reduction in the total energy consumption compared to that for single UEO. Based on the analysis of the evolution index (EI), pH was selected as the best judgment index of self-sequential UEO for indicating the time point of ultrasound irradiation, which saves irradiation times for practical use.

Received 10th January 2020

Accepted 16th March 2020

DOI: 10.1039/d0ra00285b

[rsc.li/rsc-advances](http://rsc.li/rsc-advances)

## 1. Introduction

As a primary component of non-steroidal anti-inflammatory drugs, diclofenac (DCF) is thought to be one of the emerging pollutants in the last ten years.<sup>1</sup> At present, DCF is often detected in municipal sewage influents and effluents, surface water, and groundwater.<sup>2</sup> Toxicological investigations have shown harmful effects on aquatic species even at low DCF concentrations,<sup>3,4</sup> and toxic breakdown products are formed by the degradation of DCF.<sup>5,6</sup> Accordingly, DCF must be eliminated entirely before reaching natural water.<sup>2</sup>

Ozone is a highly selective oxidant with the standard potentials of 1.25 V in basic solutions and 2.07 V in acidic solutions.<sup>7</sup> It has been extensively reported that organic contaminants are rapidly destroyed by ozonation. However, the reaction intermediates of these contaminants cannot be completely mineralized generally, which limits the broad applications of ozonation.<sup>8–10</sup> The introduction of different physical fields in ozone-based advanced oxidation processes

(AOPs), including ultrasound, ultraviolet radiation, and electricity, are practical protocols to improve the mineralization capacity of ozonation.<sup>11–13</sup> Among various protocols, previous investigations have shown that in ultrasound enhanced ozonation (UEO), the ultrasound process promotes mass transfer between ozone and the solution through agitation<sup>14</sup> as well as promotes ozone cleavage and hydrolysis through cavitation, which results in the improvement of oxidation ability through the production of more  $\cdot\text{OH}$  radicals.<sup>15</sup> Moreover, UEO has the potential advantages of being simpler, safer, and cleaner than conventional AOPs.<sup>16</sup>

It is well known that energy efficiency is one of the critical factors for the application of AOPs. The sequential reactions combine the advantages of different AOPs for improving treatment performance and promoting energy efficiency.<sup>17,18</sup> As no additional equipment is required for UEO, the  $\text{O}_3$ -UEO self-sequential treatment, which combines the degradation ability of ozonation and the mineralization ability of UEO, has been proposed for process optimization. The environment friendliness and cost-effectiveness of the  $\text{O}_3$ -UEO self-sequential treatment are determined by the time point of ultrasound irradiation, which has barely been reported. The aims of this study are (1) to study the complete degradation of DCF by ozonation and UEO and the enhanced mechanism of UEO; (2) to improve the mineralization energy efficiency using the  $\text{O}_3$ -UEO self-sequential process; and (3) to find the best judgment index for the self-sequential UEO process for indicating the time

<sup>a</sup>School of Environment and Energy, South China University of Technology, Guangzhou 510006, PR China. E-mail: [cechwei@scut.edu.cn](mailto:cechwei@scut.edu.cn)

<sup>b</sup>Guangdong Provincial Academy of Environmental Sciences, Guangzhou 510045, PR China

<sup>c</sup>School of Environment, Jinan University, Guangzhou, 510632, PR China

<sup>d</sup>Guangdong-Hongkong-Macau Joint Laboratory of Collaborative Innovation for Environmental Quality, PR China



point of ultrasound irradiation. This study offers more insights into the development of UEO for the mineralization of DCF in water, provides a feasible innovative energy-saving mode for the practical applications of combined processes, such as the O<sub>3</sub>-UEO self-sequential process, and proposes reaction control indicators to improve the operability of applications.

## 2. Materials and methods

### 2.1 Materials

Diclofenac (sodium salt), characterized by a water solubility of 237 mg L<sup>-1</sup> at 25 °C, was provided by Sinopharm Chemical Reagent Co. Ltd. (Shanghai, China). Spiked solutions with initial DCF concentrations (20 mg L<sup>-1</sup>) were prepared using water from Milli-Q equipment.

### 2.2 Experimental procedure

As shown in Fig. 1, the degradation of DCF was performed in an ultrasonic plate reactor, which was composed of stainless steel with width × height × depth of 12.0 × 24 × 12 cm. Three sides of the lower half of the reactor were installed with three series of piezoelectric transducers and were arranged in sequences at 68, 100, and 200 kHz, respectively. Three frequency generators and a power supply were in the emitting system. The maximum ultrasonic power inputs of the three fields were 200 W (68 and 100 kHz) and 180 W (200 kHz). Cold water from a cooling system was kept outside the top half of the reactor and was circulated to control the reaction temperature at about 25 °C.

Ozone was produced from O<sub>2</sub> (99.999%) through a CH-ZTW3G ozone generator (Guangzhou Chuanghuan Ozone Electric Appliance Co. Ltd., China) using the electric discharge method at 100 W. Subsequently, the ozone was fed into the reactor system with water samples through a Φ10.0 cm arc porous titanium plate (pore diameter: 0.22–100 μm, porosity:

35–50%, and bubble diameter: 0.1–2 mm) at the bottom of the reactor. In this experiment, the flow speed of ozone was 0.3 L min<sup>-1</sup>, and the ozone concentration was controlled at 32.0 mg L<sup>-1</sup>. In order to eliminate any possible side effects, the reactor should be pre-ozonated for 2 min and washed three times with distilled water. Following this, the DCF solution (3 L) was pumped into the reactor and then circulated at a rate of 0.1 L min<sup>-1</sup>. Samples were taken from the reactor at different reaction times to evaluate the multiple parameters in solution. The degradation experiments were carried out directly at an initial pH of *ca.* 6.8. All the experiments were performed in triplicate.

### 2.3 Analytical methods

DCF concentrations were determined by HPLC using a Shimadzu LC-20AT equipment, which was attached to a diode array detector and an Eclipse XDB-C18 column (4.6 mm × 150 mm, 5 μm) under isocratic elution. The mobile phase was composed of 25% of the glacial acetic acid buffer solution with 75% methanol with a flow rate of 1 mL min<sup>-1</sup>. Oxalic and oxamic acid were evaluated by Thermo TSQ Quantum Access MAX using a Waters HSS T3 column (10 cm × 2.1 mm, 1.8 μm) operating under isocratic elution of the mobile phase at a rate of 0.5 mL min<sup>-1</sup>. The mobile phase contained water and acetonitrile (volume ratio 1 : 3).

The solution pH was measured using a pH electrode (Thermo Orion model 420 A+) connected to a digital pH meter. A TOC analyzer (Vario TOC, Elementar, Germany) was used for TOC determination. The TOC detection limit was 0.03 ppm and the minimum detection concentration of TOC was 0.1 ppm. The gaseous ozone concentration was measured using the iodometric titration method. To measure the transient concentration of hydroxyl radicals produced by the decomposition of ozone, 5.0 g L<sup>-1</sup> *tert*-butanol was added to the DCF solution.

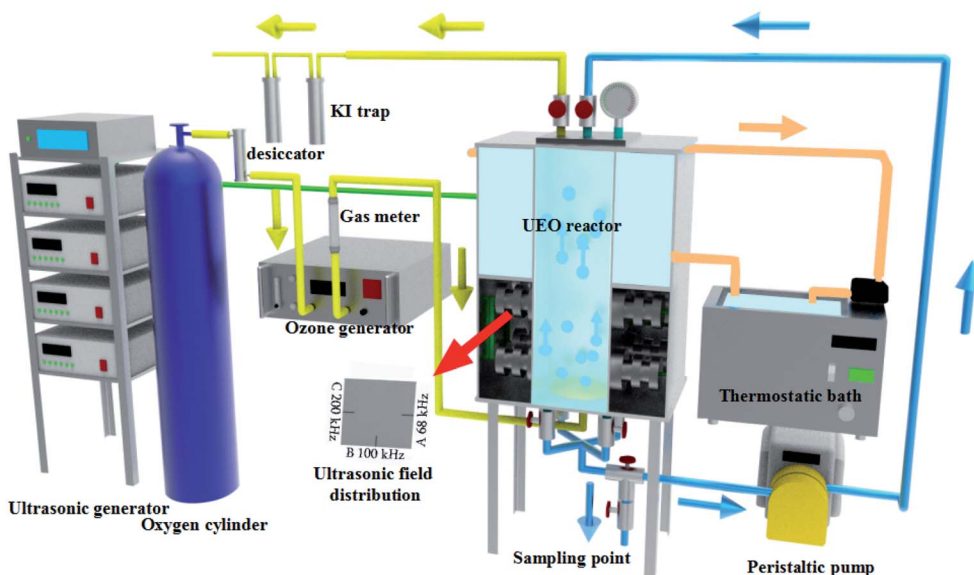


Fig. 1 Scheme of experimental facility for DCF degradation by ultrasound enhanced ozonation.

*tert*-Butanol can scavenge hydroxyl radical and produce stoichiometric formaldehyde. The concentration of formaldehyde was determined by the Hantzsch method.<sup>19,20</sup> The sample was mixed with the Hantzsch reagent and heated for 30 min at 323 K in the dark. The concentration was determined using absorbance at 412 nm ( $\epsilon = 7530 \text{ (M cm)}^{-1}$ ).

Equipped with a Dionex Ionpac CS12A column, the Dionex ICS-90 ion chromatograph was used to determine the ammonium concentration. Isocratic elution was done with  $\text{H}_2\text{SO}_4$  (11 mM) at a flow rate of  $1.2 \text{ mL min}^{-1}$ . The suppressor current was set to 90 mA. Anion concentrations were measured with a Dionex DX-600 ion chromatograph on a Dionex Ionpac AS14 column at a flow rate of  $1.5 \text{ mL min}^{-1}$ . Elution was done with  $3.5 \text{ mM Na}_2\text{CO}_3/1.0 \text{ mM NaHCO}_3$  gradient programs. The suppressor current was set at 49 mA.

### 3. Results and discussion

#### 3.1 Degradation and mineralization of DCF by ozonation and UEO

Generally, after the degradation of DCF, it is broken into other substances, while after its mineralization, it is converted to inorganic compounds, such as  $\text{H}_2\text{O}$ ,  $\text{CO}_2$ , and  $\text{NO}_3^-$ . Experiments were performed to investigate the degradation efficiency of DCF under different processes, including single ozonation and UEO (68, 100, and 200 kHz). The results are presented in Fig. 2. As shown in Fig. 2a, for all the experiments, DCF molecules were quickly degraded in less than 8 min. The introduction of ultrasound could enhance degradation slightly when compared to single ozonation. This enhancement may be due to a decrease in the liquid film thickness and an increase in the mass transfer coefficient caused by ultrasound.<sup>21</sup> Although DCF pollutants can be easily degraded by ozonation, it is difficult to mineralize DCF completely. For example, Moreira<sup>2</sup> reported that DCF (0.1 mM) was completely degraded in 5 min of ozonation, but the extent of mineralization was only 40% after 3 h. Vogna<sup>22</sup> studied DCF (1 mM) degradation by ozonation and observed complete degradation after 8 min, but the extent of mineralization was only 32% after 1.5 h.

UEO was introduced to investigate the improvement in the mineralization efficiency. In Fig. 2b, the normalized TOC ( $\text{TOC}/\text{TOC}_0$ )

as a function of time is shown for DCF ( $\text{TOC}_0 = 10.6 \text{ mg L}^{-1}$ ). The single ozonation mineralization rate reached 77% after 120 min. All ultrasound frequencies can enhance DCF mineralization, and 200 kHz UEO can lead to complete mineralization after 120 min. Hydroxyl radicals are more powerful oxidants with an electrochemical oxidation potential of 2.80 V in comparison to 2.07 V for ozone. Consequently, ozone can open aromatic compounds though its reaction with the intermediates (carboxylic acid and carbonyl compounds) is slow. Thus, these intermediates cannot be completely oxidized by molecular ozone and due to their accumulation, they become the major components of TOC residues.<sup>2,23</sup> Therefore, in this study, single ozonation was considered as a useful process for eliminating the parent compound but not the intermediates. The higher mineralization of DCF by UEO may be due to the generation of more  $\cdot\text{OH}$  radicals, which are less selective and stronger oxidants than ozone. Moreover,  $\cdot\text{OH}$  can react with the intermediates, such as small-chain organic acids. These results indicate that UEO and ozonation have different oxidation mechanisms, which need further investigation.

The first-order kinetic expression is generally used to investigate reaction kinetics due to its accuracy and simplicity.<sup>24</sup> Therefore, the following first-order kinetic expression was used to describe the DCF degradation reaction rate:

$$r = \text{d}C/\text{d}t = kKC/(1 + kC) \quad (1)$$

Here,  $C$  is the reactant concentration,  $r$  is the DCF degradation rate,  $k$  is the reaction rate constant,  $t$  is the reaction time, and  $K$  is the degradation coefficient of the reactant. When  $C_0$  is the initial reactant concentration, eqn (1) is simplified to an apparent first-order equation:

$$\ln(C_0/C) = kt \quad (2)$$

The synergy index is a quantitative way to evaluate enhanced processes<sup>4,24,25</sup> and can be defined as follows:

$$f = \frac{k_{\text{UEO}}}{k_{\text{O}} + k_{\text{U}}} \quad (3)$$

Here,  $f$  is the synergy index,  $k_{\text{UEO}}$  is the reaction rate constant for the UEO process,  $k_{\text{O}}$  is the reaction rate constant for the

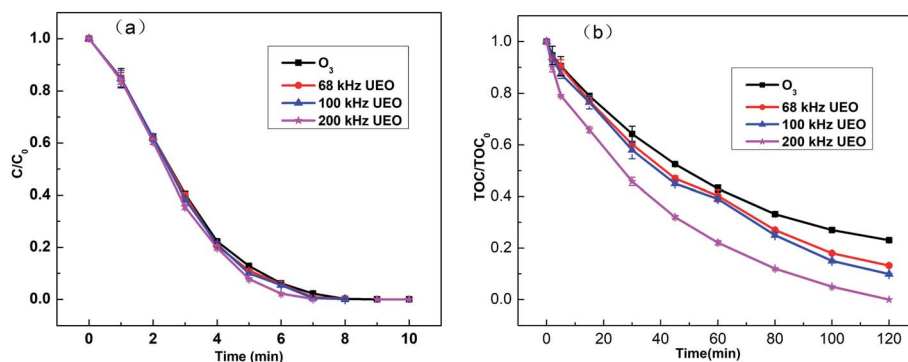


Fig. 2 (a) Normalized concentration ( $C/C_0$ ) and (b) normalized TOC content ( $\text{TOC}/\text{TOC}_0$ ) of DCF in aqueous solution ( $C_0: 20 \text{ mg L}^{-1}$ ) as a function of time.

ozonation process, and  $k_U$  is the reaction rate constant for the sonolysis process. Also,  $f > 1$  indicates that the assisting process exceeds the sum of the ozonation and sonolysis processes to achieve a synergistic degradation effect.

Based on the above-mentioned equations, the results of the degradation kinetics and synergy indices are summarized in Table 1. The rate constants  $k_U$  and  $k_{U\text{E}O}$  increased with the increase in ultrasound frequency. The synergy indices of different frequencies were between 1.17 and 1.84, and 200 kHz-UEO had the best synergistic effect (1.84), suggesting a clear synergistic effect of the UEO process.

### 3.2 Enhanced UEO mechanism

**3.2.1 Evolution of pH.** The pH of a solution indicates the concentration of hydroxyl species, which is a crucial factor affecting ozone-based AOPs. It has been extensively reported that the ozonation mechanism follows two paths: (i) attacking organic compounds selectively and directly at a low pH and (ii) undergoing decomposition by a chain reaction mechanism that produces  $\cdot\text{OH}$  at a high pH.<sup>2,26</sup> Fig. 3 shows the evolution of pH by different processes in aqueous solutions.

For all the processes, a sharp decrease in pH in the first 30 min indicated the generation of hydrogen ions and electrolysis of carboxylic acid derivatives, which was also reported by Hartmann for the degradation of diclofenac by sonolysis in the presence of catalysts.<sup>27</sup> The pH later increased because some of the carboxylic acids were mineralized to  $\text{CO}_2$  and eliminated from the saturated carbonate solution. The pH for 200 kHz UEO decreased more sharply and increased to a greater extent in comparison with that for ozonation, which indicated the stronger mineralization capacity of 200 kHz UEO. Single ozonation did not lead to a significant increase in pH at the end, which might indicate that the intermediate derivatives, such as carboxylic acid, are hardly mineralized by single ozonation due to lower  $\cdot\text{OH}$  generation at a low pH.

**3.2.2 Evolution of  $\cdot\text{OH}$  concentrations.** The generation of  $\cdot\text{OH}$  is extensively used to indicate the oxidation ability of different AOPs. The generation of  $\cdot\text{OH}$  was evaluated, as shown in Fig. 4a. For single ozonation, the generation of  $\cdot\text{OH}$  increased from 0 to 30.6  $\mu\text{mol}$  within the former 30 min and increased 12.7  $\mu\text{mol}$  within the later 90 min. This might be due to the insufficient amount of hydroxyl species, which is the critical component to form  $\cdot\text{OH}$ , as suggested by the decrease in pH.<sup>28</sup> When ultrasound was introduced, the generation of  $\cdot\text{OH}$  increased from 0 to 70.0  $\mu\text{mol}$  within the first 30 minutes and continued to increase stably throughout the rest of the treatment. The total amount of  $\cdot\text{OH}$  produced by 200 kHz UEO was 3.8 times higher than that produced by single ozonation plus

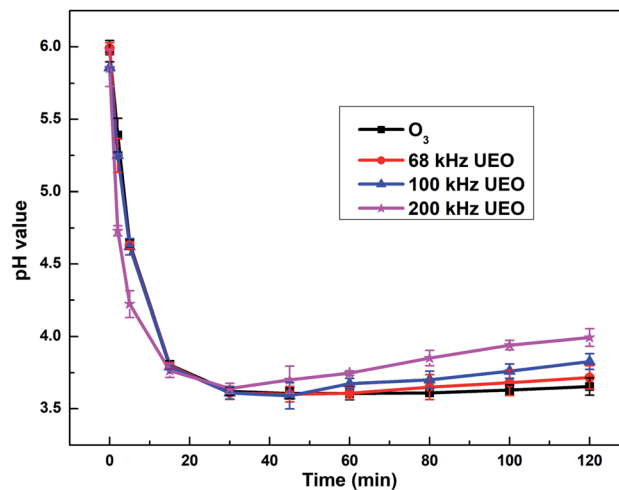
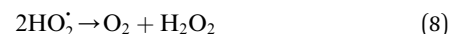
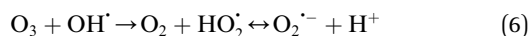
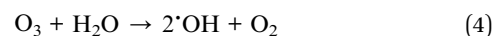


Fig. 3 Evolution of pH as a function of time.

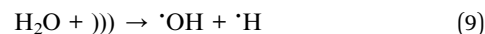
single sonolysis after 120 min. The above-mentioned results showed that the pH for UEO decreased more quickly than that for ozonation, while the  $\cdot\text{OH}$  production rate was stable at a low pH. In addition, the higher mass transfer coefficient of ozone in UEO resulted in the generation of more  $\cdot\text{OH}$  radicals. Ultrasound makes the gas bubbles of ozone turbulent. This reduces the liquid film thickness and increases the mass transfer coefficient.<sup>29</sup> Furthermore, ultrasound can crush the ozone bubbles into bubbles with larger specific surface areas.<sup>30</sup>

From the above-mentioned discussion, we can infer that  $\cdot\text{OH}$  might be generated in three ways by UEO, as shown in Fig. 4b.

(I) Ozone decomposition:<sup>7,11,16,31</sup> ozone reacts with hydroxyl groups ( $\text{pH} > 3$ ) in the same manner as that in single ozonation (eqn (4)–(8)).



(II)  $\text{H}_2\text{O}$  sonolysis:<sup>7,11,31</sup> this way is weaker than the other two ways (eqn (9)–(12)).



(III) Ozone sonolysis:<sup>7,11,31,32</sup> this way can generate radicals constantly (eqn (13)–(15)).

Table 1 Synergy indices for different processes

Ultrasound frequency (kHz)	$k_O$ ( $\text{min}^{-1}$ )	$k_U$ ( $\text{min}^{-1}$ )	$k_{U\text{E}O}$ ( $\text{min}^{-1}$ )	$f$
68	0.0135	$3.76 \times 10^{-4}$	0.0163	1.17
100		$3.43 \times 10^{-4}$	0.0175	1.26
200		$4.46 \times 10^{-4}$	0.0256	1.84

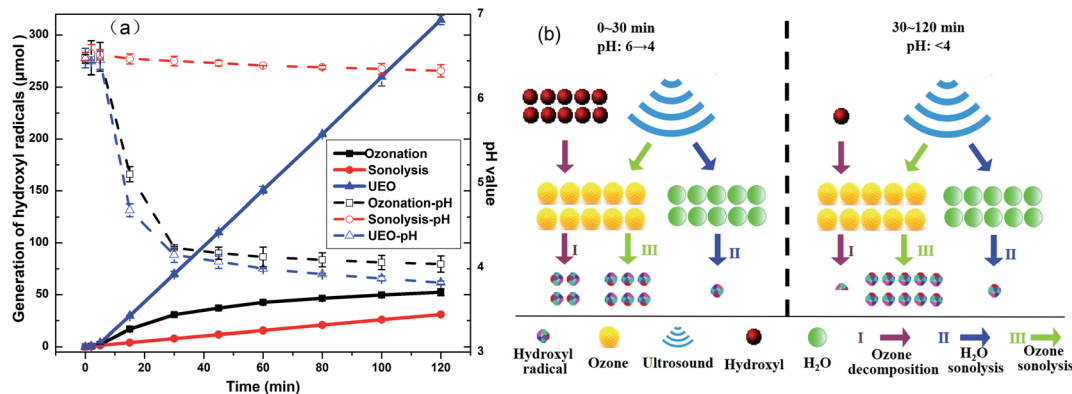
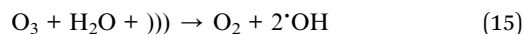
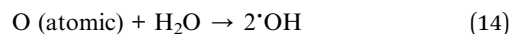
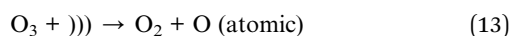


Fig. 4 (a) Generation of hydroxyl radicals and evolution of pH and (b) comparison of  $\cdot\text{OH}$  generation rate in three ways by UEO at different times and pH.



These results strongly indicate the crucial role of ultrasound, which can sonolyze H<sub>2</sub>O and ozone to increase the generation of  $\cdot\text{OH}$  even at a low pH.

**3.2.3 Evolution of intermediate products in solution.** As the typical persistent intermediates and ultimate products of nitroaromatics degradation by AOPs, oxalic acid (OXA) and oxamic acid (OMA) were selected as the representatives of low-molecular-weight carboxylic acids and used for the degradation process analysis.<sup>2,33-35</sup> The evolution of OXA and OMA concentrations is shown in Fig. 5. For single ozonation, the OXA concentration increased to 5.54 mg L<sup>-1</sup> in 30 min and decreased by ca. 37% during the remaining time. Additionally, the concentration of OXM reached 1.45 mg L<sup>-1</sup> by the end. As obtained from previous analysis, low-molecular-weight carboxylic acids are more difficult to degrade by ozone at a low pH than aromatic compounds. Faria<sup>36</sup> also found that OXA and OMA

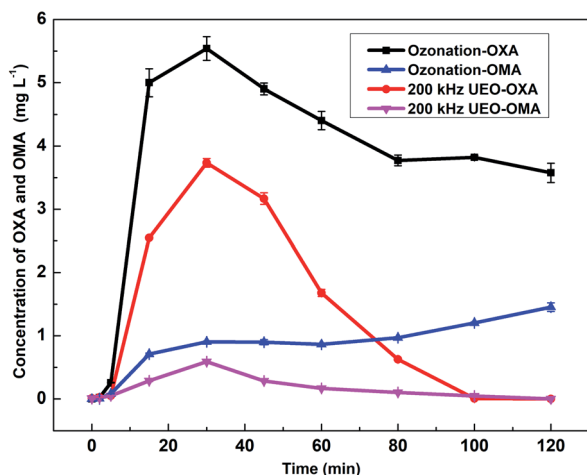


Fig. 5 Evolution of OXA and OXM in solution by ozonation and 200 kHz UEO.

were highly refractory towards ozonation at low pH (pH < 3). The OXA and OMA concentrations increased in the first 30 min and then decreased during UEO; then, all of the compounds were eliminated at the end. This might be explained by the increased  $\cdot\text{OH}$  generation by UEO. These results were also in agreement with the evolution of TOC by ozonation and UEO.

To check the evolution of nitrogen and chlorine, the normalized balance of nitrogen and chlorine is shown in Fig. 6. Nitrites were below the detection limit in all of the experiments (not shown). It was expected that nitrites (if formed) were readily transformed into nitrates in the strongly oxidizing environment. From Fig. 6a, we can infer that there is barely any generation of inorganic nitrogen in the first 5 min; then, the concentrations of nitrates and ammonium increase over the following experiment. The faster increase in the concentration of nitrates indicated the strong oxidizing capacity of UEO. Hofmann<sup>37</sup> found that ammonium was formed in stoichiometric concentrations and nitric acid and nitrous acid could not be detected *via* heterogeneous catalytic oxidation with H<sub>2</sub>O<sub>2</sub> to degrade DCF. The formation of ammonium was assumed to be a radical substitution process.  $\cdot\text{OH}$  reacted with DCF to form intermediates, such as phenol derivatives and  $\cdot\text{NH}_2$ . Then,  $\cdot\text{NH}_2$  reacted with H<sub>2</sub>O to form ammonium. Aniline derivatives were the common intermediates of DCF degradation. Then, ammonium and nitrate ions were detected in aniline derivative degradation by UEO.<sup>38</sup> Ammonium and benzoquinone were assumed to be the products of aniline degradation. As a product of aniline oxidation, nitrobenzene released nitrate during its further degradation to benzoquinone. From the above-mentioned discussion, the evolution of nitrogen in the reaction could be proposed as follows: (1) DCF was degraded to aniline derivatives; (2) aniline derivatives were degraded to benzoquinone, and ammonium was released; (3) aniline derivatives were degraded to nitrobenzene and further degradation released nitrate; (4) aniline derivatives underwent ring-opening to form nitrogen-containing acids, such as OXA, which could be further degraded to nitrate by  $\cdot\text{OH}$ .

As shown in Fig. 6b, the concentration of chlorine increases during the experiment and barely increases after 30 min. Also, 80% of dechlorination by ozonation indicated the formation of

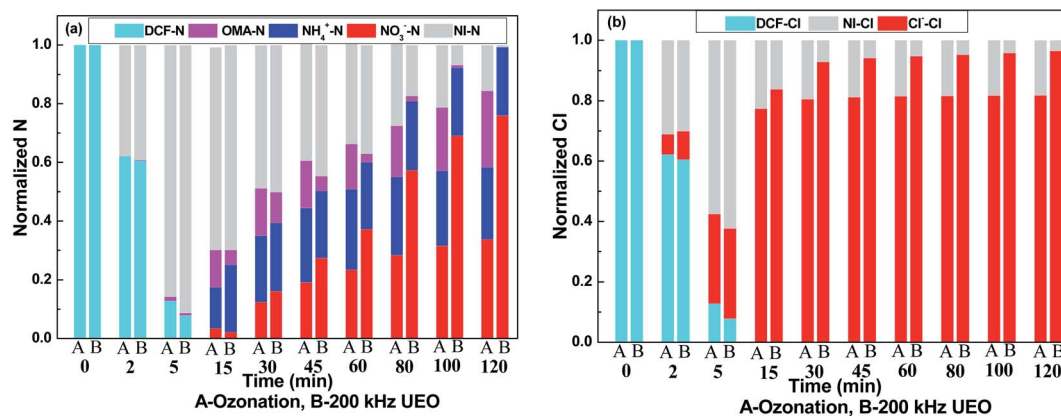


Fig. 6 Evolution of nitrogen (a) and chlorine (b) in solution.

ozone-persistent chloride, which could be degraded by the  $\cdot\text{OH}$  radicals generated by UEO. Strong dechlorination by  $\cdot\text{OH}$  and ozone was also observed by Vogna<sup>22</sup> who used UV/H<sub>2</sub>O<sub>2</sub> and ozone to oxidize DCF.

### 3.3 Mineralization energy efficiency and control indicator of the self-sequential reaction

**3.3.1 Mineralization energy efficiency of different treatments.** Energy consumption is one of the most significant reasons for high operating costs in UEO. For process optimization and promotion of energy efficiency, the O<sub>3</sub>-UEO self-sequential reaction was introduced without additional equipment. The self-sequential reaction has two steps: (1) with high energy efficiency, ozonation was used to degrade the DCF precursor and initial products; (2) UEO, which is non-selective and low pH-dependent, was introduced to further degrade the ozone-resistant intermediates for complete mineralization. The mineralization energy efficiency (MEE) was used to evaluate the energy efficiency of the reaction:<sup>33,39,40</sup>

$$\text{MEE} = \frac{(\text{TOC}_0 - \text{TOC}_t)V}{UI_{\text{O}}t + UI_{\text{U}}t} \quad (16)$$

Here, MEE is the mineralization energy efficiency ( $\text{mg} (\text{kW h})^{-1}$ ) of the reaction,  $t$  is the reaction time (min),  $\text{TOC}_0$  and  $\text{TOC}_t$  are solution TOC values at times  $t = 0$  and  $t$ , respectively ( $\text{mg L}^{-1}$ ),  $V$  is the solution volume (L),  $U$  is the average voltage (V), and  $I_{\text{O}}$

and  $I_{\text{U}}$  are the currents of ozone and ultrasound generator, respectively (A).

The MEE values of ozonation, single UEO and sequential UEO are summarized in Table 2. The results showed that ozonation had the highest MEE ( $173 \text{ mg} (\text{kW h})^{-1}$ ) without complete mineralization. Only 200 kHz sequential UEO could be used for complete mineralization. Three of the sequential UEOs led to complete mineralization, while 1 h O<sub>3</sub> followed by 1 h UEO had the best MEE ( $113 \text{ mg} (\text{kW h})^{-1}$ ), which was 37% higher than that of single 200 kHz UEO ( $82 \text{ mg} (\text{kW h})^{-1}$ ). The results show that sequential UEO is an effective treatment to save energy for complete mineralization.

**3.3.2 Control indicator of sequential reaction.** For better applying the UEO self-sequential treatment in engineering applications, the judgment index, which can indicate the time point of ultrasound irradiation, should be introduced. The evolution index (EI) was employed to evaluate the evolution rate of the reaction parameters for selecting the judgment index:

$$\text{EI} = \frac{(\text{value}_{t_2} - \text{value}_{t_1})}{\text{value}_{t_1}(t_2 - t_1)} \quad (17)$$

Here, EI is the evolution index ( $\text{min}^{-1}$ ) of the reaction parameters,  $t_1$  and  $t_2$  are the reaction times (min), and  $\text{value}_{t_1}$  and  $\text{value}_{t_2}$  are the reaction parameter values at  $t_1$  and  $t_2$ , respectively.

Table 2 The MEE of ozonation, single UEO and sequential UEO

Process	$\Delta\text{TOC}$ ( $\text{mg L}^{-1}$ )	$E$ ( $\text{kW h}$ )	MEE ( $\text{mg} (\text{kW h})^{-1}$ )	Complete mineralization	
Ozonation	8.13	0.141	173	No	
Single UEO	68 kHz UEO	0.409	72	No	
	100 kHz UEO	0.414	73	No	
	200 kHz UEO	10.57	0.418	82	Yes
	Sequential UEO	0.5 h O <sub>3</sub> + 1.5 h UEO	0.349	91	Yes
	0.75 h O <sub>3</sub> + 1.25 h UEO	0.314	101	Yes	
	1 h O <sub>3</sub> + 1 h UEO	0.279	113	Yes	
	1.33 h O <sub>3</sub> + 0.67 h UEO	0.234	126	No	
	1.67 h O <sub>3</sub> + 0.33 h UEO	0.187	144	No	

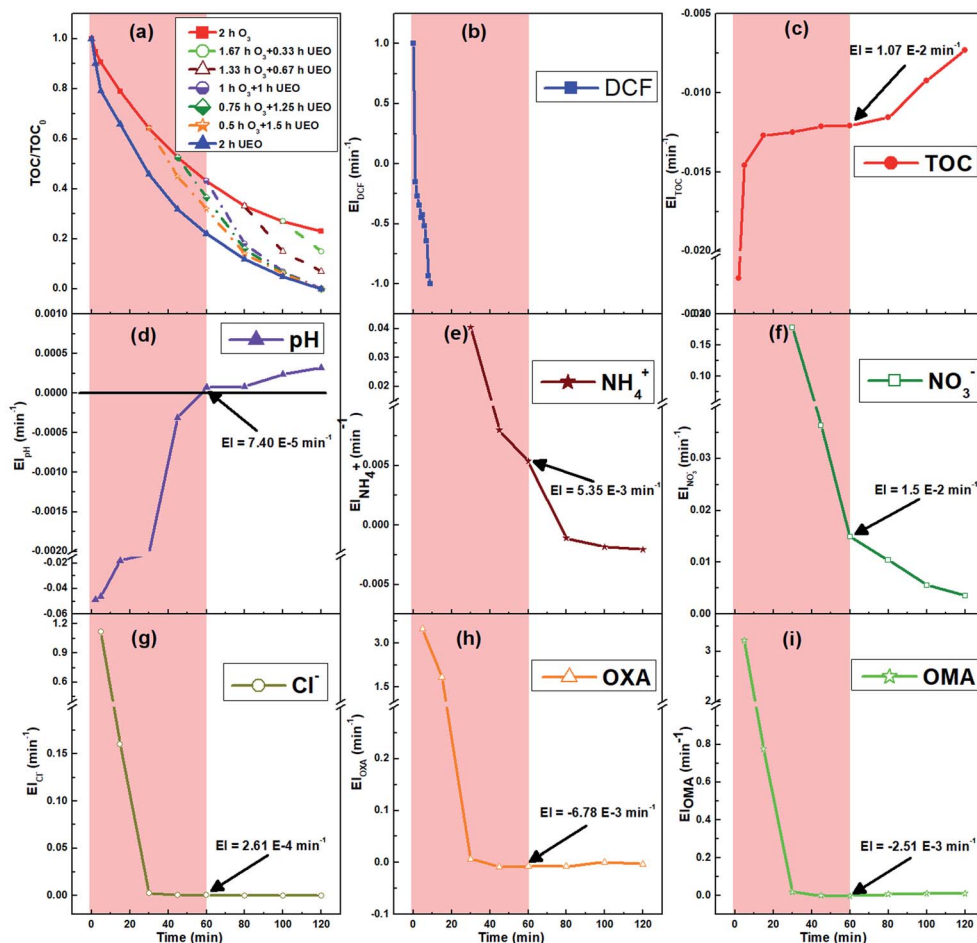


Fig. 7 The normalized TOC of self-sequential UEO (a) and the candidate judgment indices (b–i). The red area indicates the introduction time, which can ensure complete mineralization.

To intuitively compare the time points of ultrasound irradiation in different sequential UEOs and the break point of the candidate judgment indices, all results are shown in Fig. 7. From Fig. 7a, we can infer that the introduction of ultrasound before 60 min can lead to complete mineralization, and 60 min is the best time point for ultrasound irradiation. Eight candidate judgment indices were studied, as shown in Fig. 7b–i; EI<sub>DCF</sub> ends before 8 min. EI<sub>Cl<sup>-</sup></sub>, EI<sub>OXA</sub> and EI<sub>OMA</sub> barely change after 30 min. The break points of these four judgment indices are earlier than the best time point. EI<sub>TOC</sub> has a later break point, which cannot lead to complete mineralization. EI<sub>NO<sub>3</sub><sup>-</sup></sub> has no significant break point during the reaction. EI<sub>NH<sub>4</sub><sup>+</sup></sub> changes from positive to negative at the time point *ca.* 80 min, which cannot lead to complete mineralization. EI<sub>pH</sub> changes from negative to positive at the time point *ca.* 58 min, coinciding with the best time point (60 min) for ultrasound irradiation. Furthermore, pH can be quickly measured using automatic monitoring equipment in engineering applications. Thus, pH is chosen as the best judgment index of the self-sequential UEO process for indicating the time point of ultrasound irradiation.

## 4. Conclusions

In conclusion, ultrasound efficiently enhanced ozonation for the mineralization of DCF, and 200 kHz UEO was demonstrated to be the most efficient treatment for the rapid degradation and complete mineralization of DCF pollutants. UEO generated <sup>•</sup>OH through ozone decomposition, H<sub>2</sub>O sonolysis, and ozone sonolysis. Moreover, these continuously formed <sup>•</sup>OH radicals from UEO could react with ozone-resistant compounds such as OXA and OXM, resulting in complete mineralization. By reducing the ultrasound irradiation time, self-sequential UEO was demonstrated to be an energy-efficient solution for the complete mineralization of DCF. At the base of complete mineralization, the best sequential UEO (1 h O<sub>3</sub> + 1 h UEO) promoted 37% energy efficiency when compared to single UEO. Finally, based on the analysis of EI, pH was chosen as the judgment index for judging the time point of ultrasound irradiation in self-sequential UEO, which saves the irradiation time during practical applications. The present investigation provides more insights into the development of energy-saving UEO for the mineralization of organic contaminants in wastewater for practical applications.

## Conflicts of interest

There are no conflicts to declare.

## Acknowledgements

The financial support of Guangdong Province Science and Technology plan project public welfare fund and ability construction project of China (No. 2016A020221019), the National Nature Science Fund of China (No. 51878290) are greatly appreciated. This work was also supported by Special Fund Project for Science and Technology Innovation Strategy of Guangdong Province (No. 2019B121205004).

## Notes and references

- 1 M. O. Barbosa, N. F. F. Moreira, A. R. Ribeiro, M. F. R. Pereira and A. M. T. Silva, *Water Res.*, 2016, **94**, 257–279.
- 2 N. F. F. Moreira, C. A. Orge, A. R. Ribeiro, J. L. Faria, O. C. Nunes, M. F. R. Pereira and A. M. T. Silva, *Water Res.*, 2015, **87**, 87–96.
- 3 J. Schwaiger, H. Ferling, U. Mallow, H. Wintermayr and R. D. Negele, *Aquat. Toxicol.*, 2004, **68**, 141–150.
- 4 P. Finkbeiner, M. Franke, F. Anschuetz, A. Ignaszak, M. Stelter and P. Braeutigam, *Chem. Eng. J.*, 2015, **273**, 214–222.
- 5 H. Yu, E. Nie, J. Xu, S. Yan, W. J. Cooper and W. Song, *Water Res.*, 2013, **47**, 1909–1918.
- 6 L. Rizzo, S. Meric, D. Kassinos, M. Guida, F. Russo and V. Belgiorno, *Water Res.*, 2009, **43**, 979–988.
- 7 J. L. Wang and L. J. Xu, *Crit. Rev. Environ. Sci. Technol.*, 2012, **42**, 251–325.
- 8 M. M. Huber, S. Canonica, G. Park and U. von Gunten, *Environ. Sci. Technol.*, 2003, **37**, 1016–1024.
- 9 M. I. Maldonado, S. Malato, L. A. Pérez-Estrada, W. Gernjak, I. Oller, X. Doménech and J. Peral, *J. Hazard. Mater.*, 2006, **138**, 363–369.
- 10 A. Aguinaco, F. J. Beltrán, J. J. P. Sagasti and O. Gimeno, *Chem. Eng. J.*, 2014, **235**, 46–51.
- 11 R. Kidak and Ş. Doğan, *Ultrason. Sonochem.*, 2018, **40**, 131–139.
- 12 L. Bilińska, M. Gmurek and S. Ledakowicz, *Chem. Eng. J.*, 2016, **306**, 550–559.
- 13 S. Zhou, L. Bu, Z. Shi, C. Bi and Q. Yi, *Chem. Eng. J.*, 2016, **306**, 719–725.
- 14 O. Hamdaoui and E. Naffrechoux, *Ultrason. Sonochem.*, 2008, **15**, 981–987.
- 15 G. Ji, B. Zhang and Y. Wu, *J. Hazard. Mater.*, 2012, **225–226**, 1–7.
- 16 R. Poblete, I. Oller, M. I. Maldonado, Y. Luna and E. Cortes, *J. Environ. Chem. Eng.*, 2017, **5**, 114–121.
- 17 O. Gimeno, J. F. García-Araya, F. J. Beltrán, F. J. Rivas and A. Espejo, *Chem. Eng. J.*, 2016, **290**, 12–20.
- 18 P. Puspita, F. Roddick and N. Porter, *Chem. Eng. J.*, 2015, **268**, 337–347.
- 19 R. Flyunt, A. Leitzke, G. Mark, E. Mvula, E. Reisz, R. Schick and C. von Sonntag, *J. Phys. Chem. B*, 2003, **107**, 7242–7253.
- 20 F. Zhang, C. Wei, Y. Hu and H. Wu, *Sep. Purif. Technol.*, 2015, **156**, 625–635.
- 21 H. Zhang, L. Duan and D. Zhang, *J. Hazard. Mater.*, 2006, **138**, 53–59.
- 22 D. Vogna, R. Marotta, A. Napolitano, R. Andreozzi and M. D. Ischia, *Water Res.*, 2004, **38**, 414–422.
- 23 T. E. Agustina, H. M. Ang and V. K. Vareek, *J. Photochem. Photobiol., C*, 2005, **6**, 264–273.
- 24 S. F. Xiong, Z. L. Yin, Z. F. Yuan, W. B. Yan, W. Y. Yang, J. J. Liu and F. Zhang, *Ultrason. Sonochem.*, 2012, **19**, 756–761.
- 25 J. Madhavan, P. S. S. Kumar, S. Anandan, M. Zhou, F. Grieser and M. Ashokkumar, *Chemosphere*, 2010, **80**, 747–752.
- 26 S. Wang, F. Shiraishi and K. Nakano, *Chem. Eng. J.*, 2002, **87**, 261–271.
- 27 J. Hartmann, P. Bartels, U. Mau, M. Witter, W. V. Tümpling, J. Hofmann and E. Nietzschmann, *Chemosphere*, 2008, **70**, 453–461.
- 28 A. Ziylan and N. H. Ince, *Chem. Eng. J.*, 2013, **220**, 151–160.
- 29 H. Zhang, Y. Lv, F. Liu and D. Zhang, *Chem. Eng. J.*, 2008, **138**, 231–238.
- 30 T. M. Olson and P. F. Barbier, *Water Res.*, 1994, **28**, 1383–1391.
- 31 M. Gałgól, A. Przyjazny and G. Boczkaj, *Chem. Eng. J.*, 2018, **338**, 599–627.
- 32 L. K. Weavers and M. R. Hoffmann, *Environ. Sci. Technol.*, 1998, **32**, 3941–3947.
- 33 S. Garcia-Segura and E. Brillas, *Water Res.*, 2011, **45**, 2975–2984.
- 34 C. A. Orge, M. F. R. Pereira and J. L. Faria, *Chem. Eng. J.*, 2017, **318**, 247–253.
- 35 O. Rozas, C. Baeza, K. Núñez, A. Rossner, R. Urrutia and H. D. Mansilla, *Sci. Total Environ.*, 2017, **590**, 430–439.
- 36 P. C. C. Faria, J. J. M. Órfão and M. F. R. Pereira, *Appl. Catal., B*, 2008, **79**, 237–243.
- 37 J. Hofmann, U. Freier, M. Wecks and S. Hohmann, *Appl. Catal., B*, 2007, **70**, 447–451.
- 38 S. Song, Z. He and J. Chen, *Ultrason. Sonochem.*, 2007, **14**, 84–88.
- 39 H. Olvera-Vargas, N. Oturan, D. Buisson and M. A. Oturan, *Chemosphere*, 2016, **155**, 606–613.
- 40 P. Frangos, H. Wang, W. Shen, Y. Gang, S. Deng, J. Huang, B. Wang and Y. Wang, *Chem. Eng. J.*, 2015, **286**, 239–248.